Cardiovascular Toxicology (2021) 21:914–926
https://doi.org/10.1007/s12012-021-09683-w

Carbonic Anhydrase III Attenuates Hypoxia-Induced Apoptosis and Activates PI3K/Akt/mTOR Pathway in H9c2 Cardiomyocyte Cell Line

Hua Li[1] · Yibin Liu[2] · Sha Tang[1] · Jie Hu[1] · Qiuling Wu[1] · Yang Wei[1] · Ming Niu[1]

Received: 25 April 2021 / Accepted: 27 July 2021 / Published online: 13 August 2021

Abstract

Myocardial ischemia can cause insufficient oxygen and functional damage to myocardial cells. Carbonic anhydrase III (CAIII) has been found to be closely related to the abnormality of cardiomyocytes. To investigate the role of CAIII in the apoptosis of myocytes under hypoxic conditions and facilitate the strategy for treating hypoxia-induced damage, in vitro experiments in H9c2 were employed. The protein expression of CAIII in H9c2 cells after hypoxia or normoxia treatment was determined by western blotting and immunohistochemistry. MTT assay was employed for cells viability measurement and LDH release was monitored. The apoptotic cells were observed using immunofluorescence assay, flow cytometric analysis, and TUNEL assay. CAIII-overexpression or -knockdown cells were constructed to determine the role of CAIII in regulating apoptosis-related proteins caspase-3, Bax, Bcl-2, and anti-apoptosis pathway PI3K/Akt/mTOR. The mRNA levels of CAIII and genes related to CAIII synthesis including REN, IGHM, APOBEC 3F, and SKOR2 were significantly upregulated in hypoxia fetal sheep. The expression of CAIII protein and content of apoptotic H9c2 cells were increased at 1, 3, 6, and 12 h after hypoxia treatment. Overexpression of CAIII significantly upregulated Bcl2 level and downregulated Bax and caspase-3 cleavage levels, while its knockdown led to the contrary results. Overexpressed CAIII promoted the HIF-1α level and activated the PI3K/Akt/mTOR pathway, thereby exerting an inhibitory effect on hypoxia-induced apoptosis. In conclusion, our findings revealed that CAIII could protect cell from hypoxia-apoptosis of H9c2 cells, in which, activated PI3K/Akt/mTOR signaling pathway may be involved.

Keywords CAIII · Hypoxia · Apoptosis · PI3K/Akt/mTOR · H9c2 cells

Abbreviations

CAIII	Carbonic anhydrase III
AMI	Acute myocardial infarction
MI	Myocardial ischemia
CA	Carbonic anhydrase
qRT-PCR	Real-time reverse transcription quantitative PCR
FBS	Fetal bovine serum
H/N	Hypoxia/Normoxia
DAPI	4',6-Diamidino-2-phenylindole
AV/PI	Annexin V-FITC/propidium iodide
DMSO	Dimethyl sulfoxide
LDH	Lactate dehydrogenase
SD	Standard deviation
ANOVA	Analysis of variance

Handling Editor: Y. James Kang.

Hua Li and Yibin Liu are co-first authors.

✉ Hua Li
eljy09@yeah.net

[1] Cardiac Ultrasonic Department, Traditional Chinese Medicine Hospital Affiliated to Xinjiang Medical University, No. 116 Huanghe Road, Shayibake District, Ürümqi 830002, Xinjiang, China

[2] Ultrasonic Department, First Affiliated Hospital of Xinjiang Medical University, Ürümqi 830011, Xinjiang, China

Introduction

Acute myocardial infarction (AMI) caused by heart failure is one of the vital causes of sudden death worldwide [1] and can lead to severe morbidity and mortality, whereas myocardial ischemia (MI) is a common cause of AMI [2]. MI can cause insufficient oxygen and nutrient supply and

cause functional damage to myocardial cells, and then the damaged myocardial cells lead to the enlargement of the area of myocardial infarction, cardiac insufficiency, and even death [3]. More than 140 million people in the world live in high-altitude areas with thin air and low oxygen supply [4], whereas hypoxia can cause serious damage to various tissues and organs, including the heart [5]. Therefore, a better understanding of the molecular pathogenesis of cardiomyocyte injury is the key to preventing myocardial injury and treating acute myocardial infarction. As a soluble protease in the cytoplasm, carbonic anhydrase III (CAIII) is a special member of the family and has its unique features in terms of tissue distribution, molecular structure, and biological function compared with other carbonic anhydrase (CA) isozymes [6].

CAs are a family of zinc-containing metalloproteinases that can reversibly and efficiently catalyze the hydration reaction of CO_2. So far, 13 CA isozymes have been found in mammals. They are the main participants in many physiological processes, including renal and male reproductive tract acidification, signal transduction, and gastric acid formation [7]. The current clinical research on CAIII is mainly limited to the use of the special distribution of CAIII in human skeletal muscle to explore its relationship with muscle diseases [8], suggesting that CAIII might become a new marker of muscle disease. With the further research of CAIII, it has been found that CAIII may be closely related to the abnormality of cardiomyocytes, for excessive muscle fatigue can easily cause cardiomyocytes to be hypoxic, and thus cause irreversible damage to cardiomyocytes [8]. In addition, the clinical diagnosis now uses the ratio of myoglobin/carbonic anhydrase III as an early diagnosis of myocardial injury during acute myocardial infarction [9], while the exact physiological role of CAIII in myocardial infarction is still unclear. Further research indicates that CAIII may be significantly related to the apoptosis of muscle cells. Ren et al. found that CAIII protein levels in skeletal muscle of patients with myasthenia gravis were significantly lower than those in normal people [10]. Shang et al. found that CAIII overexpression could effectively reduce the apoptosis rate of C2C12 (a mouse skeletal muscle cell line) cells [8]. Another study showed that the mRNA content of the lateral femoral muscle CAIII in the hypoxic training group was 74% higher than that in the normoxic training group [11]. These studies indicate that CAIII may be involved in the apoptosis of myocytes under hypoxic conditions, thereby improving myocyte status. The PI3K/Akt/mTOR signal transduction pathway is an important signal pathway for protein synthesis in the body and plays an important role in regulating cell proliferation, differentiation, and apoptosis [12, 13].

Based on these findings, we hypothesized that CAIII could protect cardiomyocytes from hypoxia-induced cardiomyocyte damage. However, to date, there has been no research on the protective mechanism of CAIII in hypoxic cardiomyocytes. Hence, we aimed to investigate the changes in the level of CAIII in hypoxic cardiomyocytes, the effect of changes in the level of CAIII on cardiomyocyte apoptosis, and its relations with the PI3K/Akt/mTOR signaling pathway.

Methods

Animal Feeding and Modeling

Sixteen normal pregnant sheep (body weight 25–35 kg, about 10 months of age, CL) successfully bred by sexual maturity artificial insemination were randomly divided into 2 groups ($n = 8$): normoxia group and hypoxia group. The special environment artificial simulation experiment chamber (DYC-3010M) was used to adjust the parameters of the artificial experiment chamber to accurately simulate the low-oxygen climate environment on the plain and plateau. Normoxia group's sheep were raised in a plain environment (temperature for 20 °C, humidity for 11.0 g/m^3, O_2 content for 260 g/m^3, pressure for 100.0 kPa), and hypoxia group's sheep were simulated in low-pressure alpine environment with an altitude of 3000 m (temperature for 5 °C, humidity for 3.68 g/m^3, O_2 content for 206 g/m^3, pressure for 67.7 kPa). During the breeding period, the animals drunk water and ate freely. The cabin was opened every 24 h to add water and feed. The breeding in the cabin lasted throughout the gestation period. Since very high doses of propofol can cause sudden arrhythmias and refractory with circulatory collapse in some animals, it is recommended that infusing low doses of ketamine intravenously to reduce the total amount of propofol. Besides, isoflurane was used to assist in maintaining anesthesia because isoflurane can promote a low Vt (Tidal volume) and less influence of propofol the neuro-ventilatory efficiency [14]. After the feeding cycle, the maternal sheep of each group were anesthetized using ketamine (10 mg/kg) with a bolus intramuscular injection and propofol (2–6 mg/kg) with a bolus intravenous injection as previously described [15–19], for their potent analgesic and favorable anesthetic properties, and maintained with isoflurane (1–3%) by inhalation and propofol by intravenous injection. The fetal sheep were removed from maternal sheep via laparotomy and maternal sheep were euthanized through intravenous injection of pentobarbital (160 mg/kg). Subsequently, according to the confirmation policy of euthanasia (IACUC, institutional animal care and use committee, https://animal.research.uiowa.edu/iacuc-policy-confirmation-euthanasia), bilateral thoracotomy, sternotomy, and removal of heart and lungs were performed to ensure the death of the pregnant sheep. For the fetal sheep,

according to the Council Regulation (EC) No 1099/2009 on the protection of animals at the time of killing (https://eur-lex.europa.eu/eli/reg/2009/1099/oj), the head-to-body electrical stunning with 1 A was applied on the fetal sheep to ensure unconsciousness, and then the heart of the fetal sheep was removed. Then apical 2 mm^3 myocardial tissue of each group of fetal sheep was quickly cut off for immunohistochemical analysis. This study was approved by the Ethics Committee of General Hospital of Xinjiang Military Region of the People's Liberation Army (No. 2017.301).

Real-Time Reverse Transcription Quantitative PCR (qRT-PCR)

50–100 mg of myocardial tissue was washed with cold PBS pH 7.4 and stored in RNAlater® (AmbionTM) at 4 °C. Total RNA was extracted with TRIpure Isolation Reagent® Kit (Thermo Fisher, Waltham, USA), treated with DNase I (RNase-free) (Thermo Fisher, Waltham, USA), then its integrity was verified by 1% agarose gel electrophoresis. The samples were stored at − 80 °C and cDNA synthesis was then performed using the High Capacity cDNA Reverse Transcription® (Applied Biosystems™) kit according to the manufacturer's protocol, and their quantity and purity were evaluated. The reverse transcription product of cDNA was stored at − 20 °C. Then quantitative PCR (qRT-PCR) was applied using ABI7500 Real-Time qPCR real-time fluorescence reaction system to measure the relative RNA level using the Power SYBR® Green PCR Master Mix (Thermo Fisher, Waltham, USA) on a StepOne Real-Time PCR system under the following conditions: 10 min 95 °C, 35 cycles of 10 s 95 °C, 30 s 60 °C, and finally 30 s 72 °C. The specific primers used in qRT-PCR are available in Table 1. The levels of target genes were normalized to the level of internal GAPDH using the $2^{-\Delta\Delta Ct}$ method.

Table 1 The primers of detected mRNA

	Primers (5' → 3')
GAPDH	Forward: TTTGAGGGTGCAGCGAACTT
	Reverse: ACAGCAACAGGGTGGTGGAC
Ren	Forward: CCTGTGGTCCTCACCAACTA
	Reverse: AGGATTCCAGGGAGTCGTAG
IGHM	Forward: TGTTCAAGGTGAAGTGACGG
	Reverse: GATGCGGGGAAGATTTCAGT
APOBEC3F	Forward: GCCTTGGAAGAAACTGAAGAG
	Reverse: GTCAAGCATCAAGTCGTCAAG
CAIII	Forward: CTGAAAGCAACTTCCAAGCAA
	Reverse: CCCTAACCTAGAGCCGAAGT
SKOR2	Forward: GTGCCCATCTCAGCAAAAGC
	Reverse: CATTTGCAGTCTCTGTGCGG

Cell Cultures

The H9c2 cells were provided by Stem Cell Bank, Chinese Academy of Sciences (Shanghai, China). Then, 0.125% trypsin–EDTA and 0.1% collagenase were used to digest heart tissues. The cells were cultured in the medium at 37 °C in a humidified incubator with 5% CO_2 as following formula: DMEM containing 10% fetal bovine serum (FBS), 100 U/mL penicillin/streptomycin. The cells were preliminarily seeded into culture bottle at a density of 1×10^5/mL and incubated for 72 h before the subsequent experiments.

Hypoxia/Normoxia (H/N) Model

The in vitro cardiomyocyte hypoxia/normoxia (H/N) model used in our study was constructed according to a previous publication [20]. The hypoxia group was induced by exposing cardiomyocytes to 95% N_2 and 5% CO_2 at 37 °C. The normoxia group was incubated in the normal cell chamber with no extra treatment. All experiments undergoing H/N treatment were repeated in triplicate.

Immunofluorescence Assay

H9c2 cells were preliminarily seeded into 24-well plates at a density of 1×10^5 cells/well and incubated for 24 h and then undergoing H/N treatment. After that, cells were prefixed in 4% paraformaldehyde and permeabilized with 0.1% Triton X-100 at room temperature for 20 min and fixed in cold methanol at − 20 °C for 10 min. For the detection of CAIII level (Fig. 2B), cells were incubated with primary antibodies for anti-CAIII (1:500, Abcam, MA, USA) and 4',6-diamidino-2-phenylindole (DAPI) (1:1000, Abcam, MA, USA) at 4 °C overnight. Then the cells were incubated with goat anti-rabbit IgG-Alexa Fluor 555 antibodies (1:500, Abcam, MA, USA) at 37 °C for 1 h. The expression of CAIII in cells was visualized by fluorescence microscope (Olympus, Tokyo, Japan).

Plasmid Construction and Cell Transfection

The target gene and the vector PLVshRNA-EGFP (2A) Puro were double-digested with endonucleases BamH I and EcoR1. After amplification of the target gene, the restriction sites of EcoR1 and BamH I were introduced at both ends of the primer. Then, the plasmid vector PEGFP-C1 and the target gene were digested with EcoR1 and BamH I and then ligated, transformed, and identified. All the used vector, CAIII(+), sh-CAIII, and sh-NC plasmids were constructed at the GenePharma Co., Ltd. (Shanghai, China). The H9c2

cells were seeded into 12-well plates with DMEM medium 24 h before transfection. Transfection of target genes was implemented when the fusion of cells reached to 90%. About 0.8 μg of each plasmid DNA and 2.0 μL of Lipofectamine® 2000 transfection reagent (Invitrogen, Carlsbad, CA, USA) were diluted by 50 μL of Opti-MEM, respectively. The diluted DNA and transfection reagent were mixed up to form the transfection complexes and maintained at room temperature for 20 min, after which the mixture was immediately added into cells to transfect for 6 h at 37 °C in a 5% CO_2 atmosphere. The original medium was then replaced with fresh complete medium containing 10% FBS and further incubated for 24 h. The cells were washed PBS twice and cultured in G418 medium, and the fresh screening medium was changed every 2–3 days. Finally, the green fluorescence was observed under microscope to obtain the successfully transfected cells.

Western Blotting

Proteins were extracted from 0.2 g of myocardial tissue and separated by SDS-PAGE and then transferred to a PVDF membrane. After the membrane was washed, it was placed in the anti-CAIII (ab181358, Abcam, MA, USA, 1:1000), anti-HIF-1α (ab228649, Abcam, 1:1000), anti-cleaved Caspase-3 (ab49822, Abcam, 1:1000), anti-Bcl-2 (ab194583, Abcam, 1:1000), anti-Bax (ab32503, Abcam, 1:500), anti-p-PI3K (PA5-37820, Thermo Fisher, 1:1000), anti-t-PI3K (#4257, Cell Signaling Technology, 1:1000), anti-p-Akt (#9271S, Cell Signaling Technology, 1:1000), anti-t-Akt (ab179463, Abcam, 1:1000), anti-p-mTOR (#5536, Cell Signaling Technology, 1:1000), anti-t-mTOR (ab32028, Abcam, 1:1000), anti-p-p70S6K^{Thr389} (AF5899, Beyotime, Shanghai, China, 1:1000), anti-t-p70S6K (3485-100, BioVision, Shanghai, China, 1:1000), and anti-β-actin (ab179467, Abcam, 1:1000) primary antibody at 4 °C overnight, and then the membrane was rinsed and added to the Goat Anti-Rabbit IgG secondary antibody and incubated at room temperature for 2 h. Then it was put into the mixed color development solution to develop color, and finally the reaction was stopped. Image analyzer quantitative system was used for density analysis, and β-actin was used as an internal reference.

Immunohistochemistry

The myocardial tissue was prepared into paraffin tissue sections of about 4 μm. After dewaxing, hydration, and blocking of endogenous enzymes, sections were blocked with goat serum for 2 h and then rewarmed at room temperature. Rabbit anti-human CAIII polyclonal antibody (1:100, Santa Cruz, Shanghai, China) was added and incubated for 30 min. After washing with PBS, non-biotinylated IgG was added and incubated at 37 °C for 20 min. After adding DAB staining solution (Solarbio, Shanghai, China), hematoxylin was used to re-dye for 2 min, dehydrated by gradient alcohol and dried naturally, and then sealed with neutral gum; the protein expression in each tissue was observed by microscopy. Image-Pro Plus (Version 6.0; Media Cybernetics, Silver Spring, MD, USA) was used to quantify the relative level of the stains.

TUNEL Assay

The constructed H9c2 cells were preliminarily seeded into 24-well plates at 1×10^5 cells/well and incubated for 24 h and then undergoing H/N treatment for 24 h. Cells were subsequently prefixed with 4% paraformaldehyde in 0.1 mol/L PBS for 1 h at 25 °C. After rinsing with PBS, 1% Triton X-100 was used for cells' permeabilization. Then the DNA fragments that broke during cell apoptosis were detected using a TUNEL detection kit (Roche Clinical Laboratories, Indianapolis, USA). DAPI (Abcam, MA, USA) was obtained for nuclear staining. Apoptotic cells were examined under a fluorescence microscope.

Flow Cytometric Analysis

H9c2 cells were preliminarily seeded into 24-well plates at a density of 1×10^5 cells/well and incubated for 24 h and then undergoing H/N treatment. The content of apoptotic cells was detected by annexin V-FITC/propidium iodide (AV/PI) dual staining according to the manufacturer's instructions, and then results were determined via a flow cytometer (BD Bioscience, CA, USA).

MTT Assay

To determine the cell viability, MTT assay kit (Beyotime, Haimen, China) was implemented. After H/N treatment for 24 h, MTT solution (5 mg/mL, dissolved in fresh serum-free medium) was added into each well, and cells were incubated for another 4 h at 37 °C. After removing the supernatant, 100 μl of dimethyl sulfoxide (DMSO) was added to dissolve the resulted formazan crystals completely. A microplate reader (Thermo Fisher, MA, USA) was obtained for monitoring the OD570 value. The cell viability (%) was calculated as a percentage relative to the absorbance of control cells with normoxia treatment.

Detection for LDH Activity

After H/N treatment, the level of lactate dehydrogenase (LDH) was determined using Cytotoxicity Assay Commercial kits from Nanjing Jiancheng Bioengineering Ltd. (Shanghai, China) for evaluation of cardiomyocyte injury

[21]. A microplate reader (Thermo Fisher, MA, USA) was obtained for monitoring the OD490 value.

Statistical Analysis

All the tests were performed in triplicates and all data were presented as the means ± standard deviation (SD). GraphPad Prism 7.0 (software, CA, USA) was taken for the data analysis. The comparisons among multiple groups were made with one-way (one factor and multiple levels) or two-way (two factors and multiple levels) analysis of variance (ANOVA) followed by Tukey's test. Student's *t* test was employed to analyze the comparison between two groups. The difference at the value of $P < 0.05$ or $P < 0.01$ was considered statistically significant ($^{*}P < 0.05$, $^{**}P < 0.01$).

Results

Hypoxia Promoted CAIII Level in Sheep Heart Tissue

Our previous studies showed that hypoxia would cause damage to the heart of prenatal sheep, and proteomics results presented the significant differential expression of CAIII, REN, IGHM, APOBEC 3F, and SKOR2 protein in heart tissue of hypoxic group compared with normal group [22]. The qRT-PCR method was used to verify the mRNA expression of CAIII (Fig. 1A). The consistent result showed that CAIII was significantly up-regulated in the hypoxia group of myocardial tissue than that in the normoxia group (Fig. 1A). From the results of western blotting (Fig. 1B), it could be seen that the expression of CAIII in hypoxia group was significantly increased ($P < 0.01$). Further immunohistochemical results (Fig. 1C) also showed that the protein expression of CAIII in the hypoxia group was obviously higher than that in the normoxia group ($P < 0.01$) and CAIII was

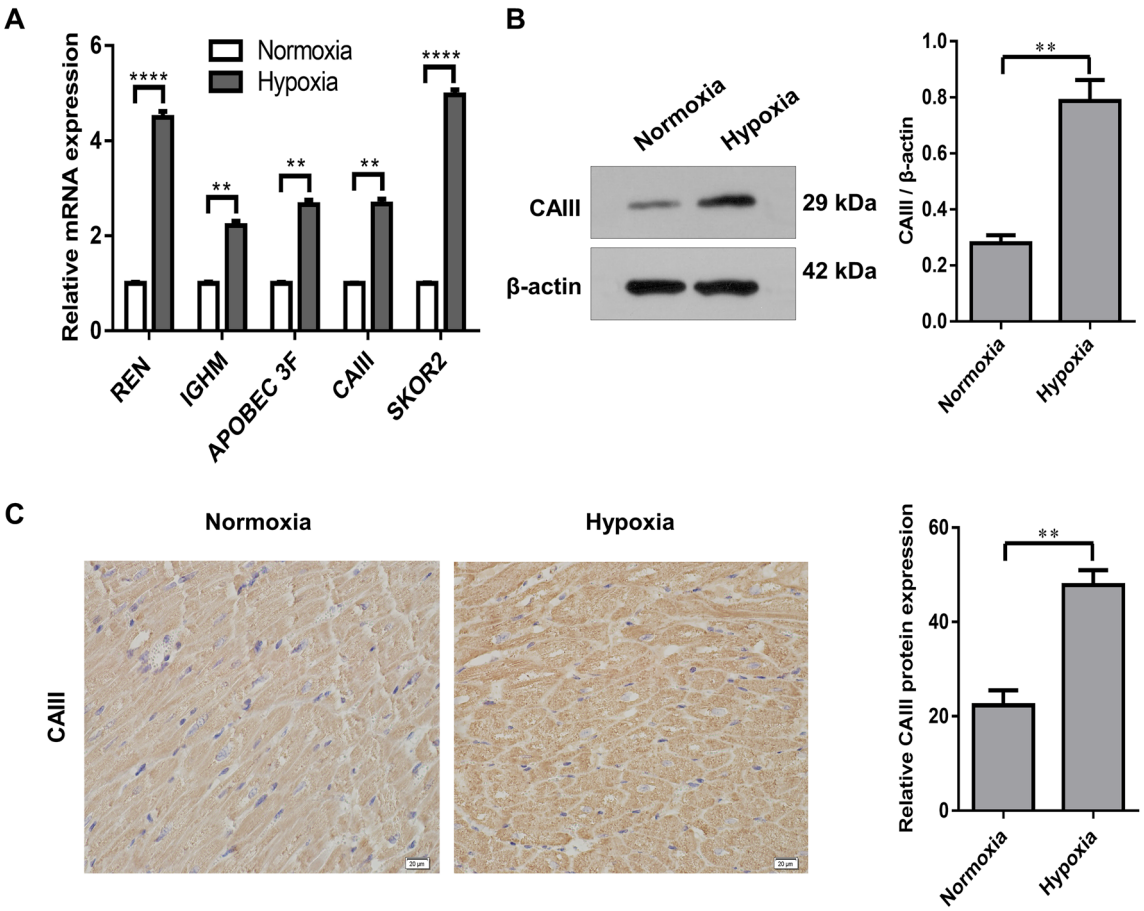

Fig. 1 The qPCR technology to verify proteomics of myocardial tissue in prenatal hypoxic fetal sheep. **A** Expression of genes related to CAIII synthesis in myocardial tissues, including REN, IGHM, APOBEC 3F, CAIII, SKOR2. **B** Hypoxia affected the protein expression of CAIII gene in myocardial tissue detected by western blotting. **C** Hypoxia affected the protein expression of CAIII gene in myocardial tissue detected by immunohistochemistry. $n = 8$, $^{*}P < 0.05$, $^{**}P < 0.01$, $^{****}P < 0.0001$ versus normoxia group

mainly expressed in the cytoplasm. These results indicated that CAIII expression in myocardial tissue was significantly enhanced under hypoxic conditions.

Hypoxia Increased CAIII Level in H9c2 Cells

In order to determine the impact of hypoxia on the expression of CAIII in H9c2 cells, western blotting and immunofluorescence analysis were performed. As shown in Fig. 2A, the expression of CAIII was significantly upregulated by hypoxia in a time-dependent manner compared with normoxia group ($P < 0.05$). The level of CAIII with 6 h hypoxia was higher than that with 3 h hypoxia. When the hypoxia treatment last for 12 h, the expression of CAIII was increased to almost threefold of that in normoxia group. The consistent result was exhibited in immunofluorescence graphs (Fig. 2B). The 12 h hypoxia treatment also increased the amount of apoptotic H9c2 cells (Fig. 2C), indicating that CAIII might participate in the apoptosis of cells in hypoxia environment ($P < 0.01$).

Overexpression or Silence of CAIII in H9c2 Cells

To determine the function of CAIII in H9c2 cells, the vector, CAIII(+), sh-CAIII, and sh-NC plasmids were constructed and transfected. Observation under microscope directly reflected that the plasmids were successfully transfected into > 95% of the H9c2 cells (Fig. 3A). As presented in Fig. 3B and C, the protein and mRNA levels of CAIII were significantly increased in CAIII(+) group compared with Control + vector groups ($P < 0.01$), while those were significantly decreased in sh-CAIII group compared with Control + vector, sh-NC, and Control group ($P < 0.01$). All these data showed that overexpression/silence systems of CAIII were successfully constructed for the subsequent experiments.

Overexpression of CAIII Prevented Hypoxia-Induced Viability Decline and Apoptosis in H9c2 Cells

After hypoxia treatment for 24 h, the CAIII level was significantly upregulated in CAIII(+) group and downregulated in sh-CAIII group compared with the normoxia group (Fig. 4A) ($P < 0.01$). Hypoxia treatment reduced H9c2 cells' viability and increased the LDH release compared with the normoxia group (Fig. 4B, C) ($P < 0.01$). However, the overexpression of CAIII in CAIII(+) group alleviated the hypoxia-induced injury effects, while silence of CAIII in sh-CAIII group no longer exhibited protective function due to reduced cell viability compared with hypoxia control group. The TUNEL results which represented the content of apoptotic cells were consistent with the results above (Fig. 4D). These evidences all suggested that CAIII in H9c2 cells could prevent hypoxia-induced viability decline and cell apoptosis.

Overexpression of CAIII Alleviated Hypoxia-Induced Cell Apoptosis Through Regulating Related Proteins

Our findings through flow cytometric analysis (Fig. 5A) indicated that 24 h treatment of hypoxia caused more obvious cell apoptosis compared with normoxia group. Interestingly, this pro-apoptotic effect was remarkably reduced by overexpression of CAIII ($P < 0.05$). Then, western blotting was performed to detect apoptosis-related proteins, including Bcl-2 that belongs to anti-apoptotic proteins, whereas Bax and caspase-3 that belong to pro-apoptotic proteins [23]. As shown in Fig. 5B, the level of Bcl-2 was dramatically upregulated, while Bax and caspase-3 were downregulated by hypoxia treatment, which was attenuated by overexpression of CAIII ($P < 0.05$). Moreover, these effects could be greatly reversed when the expression of CAIII was inhibited using sh-CAIII.

Overexpression of CAIII Activated PI3K/Akt/mTOR Pathway

Results in Fig. 6A illustrated that the level of HIF-1α was increased and the proportion of p-PI3K, p-Akt, p-mTOR, and p-p70S6K to their total forms were decreased after hypoxia treatment ($P < 0.05$). The overexpression of CAIII significantly upregulated the expression of HIF-1α compared with hypoxia + vector group; however, no significant difference in HIF-1α expression was observed between normoxia + vector and normoxia + CAIII(+) group. Consistently, overexpression of CAIII could enhance the proportion of p-PI3K, p-Akt, p-mTOR, and p-p70S6K. Furthermore, we found that the apoptosis of H9c2 cells was significantly increased under treatment with the specific mTOR inhibitor rapamycin (Fig. 6B). These results indicated that PI3K/Akt/mTOR pathway might play an essential role in regulation of CAIII-mediated attenuation of hypoxia-induced apoptosis.

Discussion

Hypoxia refers to a series of pathological processes in the metabolism, function, and morphological structure of tissues. These processes cause abnormal changes due to insufficient oxygen supply, which has been reported to occur in brain cells, skeletal muscle cells, and cardiomyocytes. A recent study found that the expression of enzymes such as calcium-dependent calmodulin kinase II was upregulated in rats with myocardial injuries that was induced by chronic intermittent hypoxia [24]. High concentrations of CAIII in muscle had a variety of biological activities that could

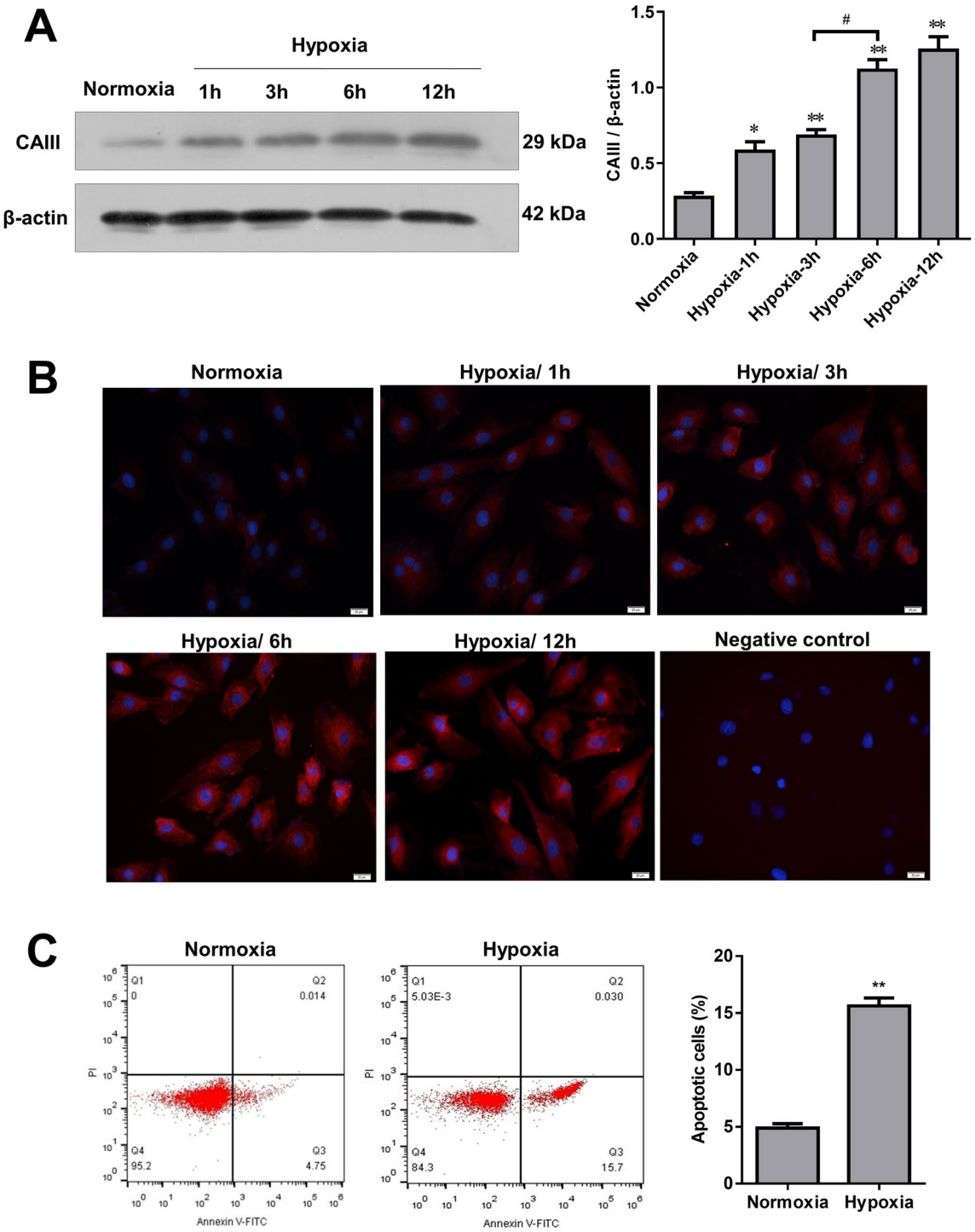

Fig. 2 Expression of CAIII was detected in normoxia group and 1, 3, 6, 12 h of hypoxia treatment group. **A** Expression of CAIII protein was determined by western blotting. The relative expression was calculated via normalization to β-actin expression. **B** The CAIII protein expression was observed by immunofluorescence assay (bar = 20 μm). Red dots referred to CAIII proteins and blue dots referred to living H9c2 cells. **C** The content of apoptotic H9c2 cells was determined by flow cytometric analysis (*$P < 0.05$, **$P < 0.01$ vs. normoxia group, $^{\#}P < 0.05$ between two groups)

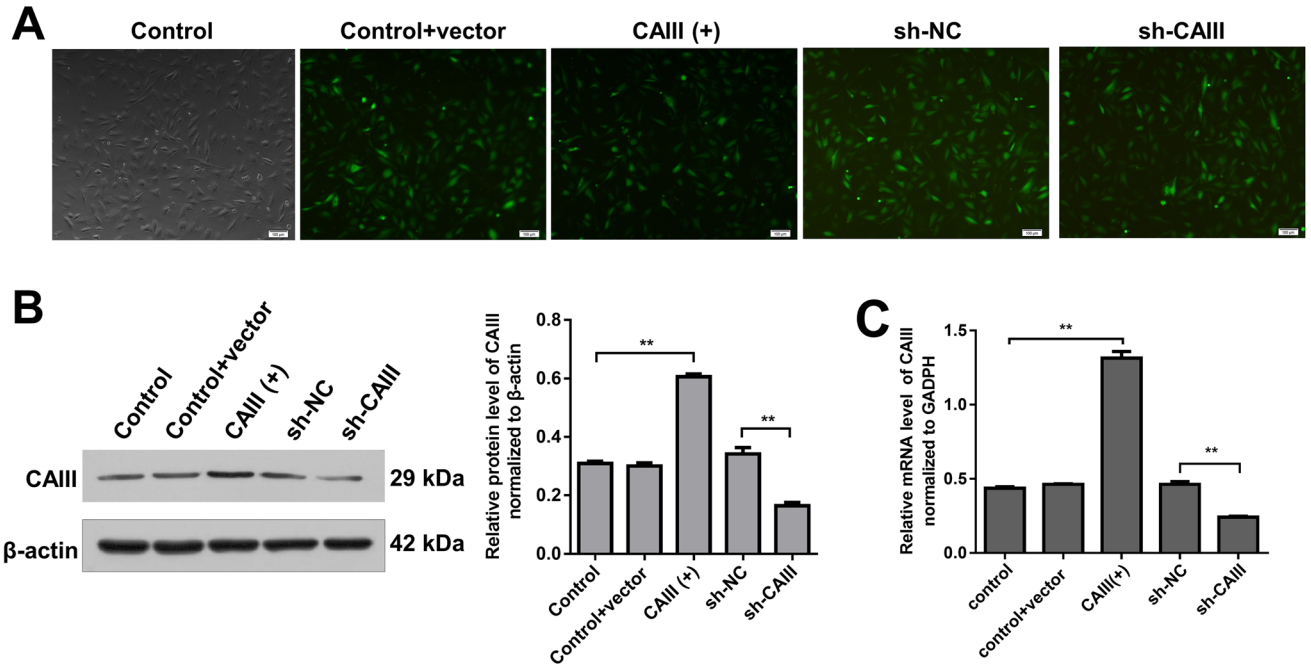

Fig. 3 Expression of CAIII was detected in control, control + vector, CAIII(+), sh-NC, and sh-CAIII group**. A** Transfection of vectors was observed by fluorescence microscope (scale bar = 100 μm). **B** Expression of CAIII protein was detected by western blotting. The relative expression was calculated via normalized to β-actin expression. **C** mRNA level of CAIII was detected by western blotting. The relative expression was normalized to GAPDH level. Green dots referred to vectors that were successfully transfected into H9c2 cells (*$P < 0.05$, **$P < 0.01$)

dispel or resist some fatigue-related substances [8]. CAIII has been reported to be gradually increased during muscle aging [25]. The activity of CAIII in serum was considered to be measured while measuring myoglobin content to distinguish damaged cardiomyocytes from other muscle cells, so that patients with myocardial infarction could be diagnosed within a few hours [26]. However, few studies have focused on their expression and role in myocardial tissues undergoing hypoxia. Since CAIII is very abundant in skeletal muscle cytoplasm and the myocardial CAIII content is very low compared with skeletal muscle, if the expression of CAIII in myocardial tissue or cells increases abnormally, the degree of myocardial damage can be judged according to the amount of its expression.

Our previous research showed that prenatal hypoxia would have a significant effect on the development of the fetal sheep's heart, causing myocardial tissue edema and abnormal mitochondrial distribution, thereby further causing cardiomyocyte apoptosis [22]. The proteomic results indicated that the CAIII, an important enzyme participated in multiple biological processes, was upregulated in myocardial tissues of prenatal hypoxic fetal sheep [22]. Interestingly, it was hypothesized that the body could upregulate the expression of CAIII for stimulus defense when confronted with hypoxia circumstance. Therefore, exploring the changes in CAIII expression in the case of myocardial tissue injury is necessary to understand the mechanism of myocardial injury.

In previous investigation, hypoxia was found to participate in inducing apoptosis of cardiac fibroblasts [27] and human pulmonary artery smooth muscle cells [28]. The content of apoptotic slow skeletal muscles cells was decreased after enhancing CAIII expression [29]. Consistently, TUNEL assay and flow cytometric analysis implemented in this study showed that the apoptotic H9c2 cells were significantly increased after hypoxia treatment, while overexpression of CAIII could attenuate the apoptosis. During hypoxia-induced apoptosis of human osteosarcoma cells, the expression of Bcl-2, an anti-apoptotic protein, was suppressed. The treatment of adrenomedullin could block cell apoptosis and enhance the level of Bcl-2 [30]. The miR-133b-5p could contribute to the protection of cardiomyocytes by inhibiting the activation of pro-apoptotic proteins such as Bax and cleaved caspase-3 [31]. Wagdy et al. found that inhibition of CAIII could reduce Bcl-2 expression and upregulate capase-3 level [32]. Our findings also showed that overexpression of CAIII could increase the Bcl-2 level and decrease Bax and capase-3 level, suggesting that CAIII might alleviated hypoxia-induced cell apoptosis through regulating apoptosis-related proteins.

HIF-1α is a nuclear protein with transcriptional activity and has a fairly broad target gene spectrum, including nearly

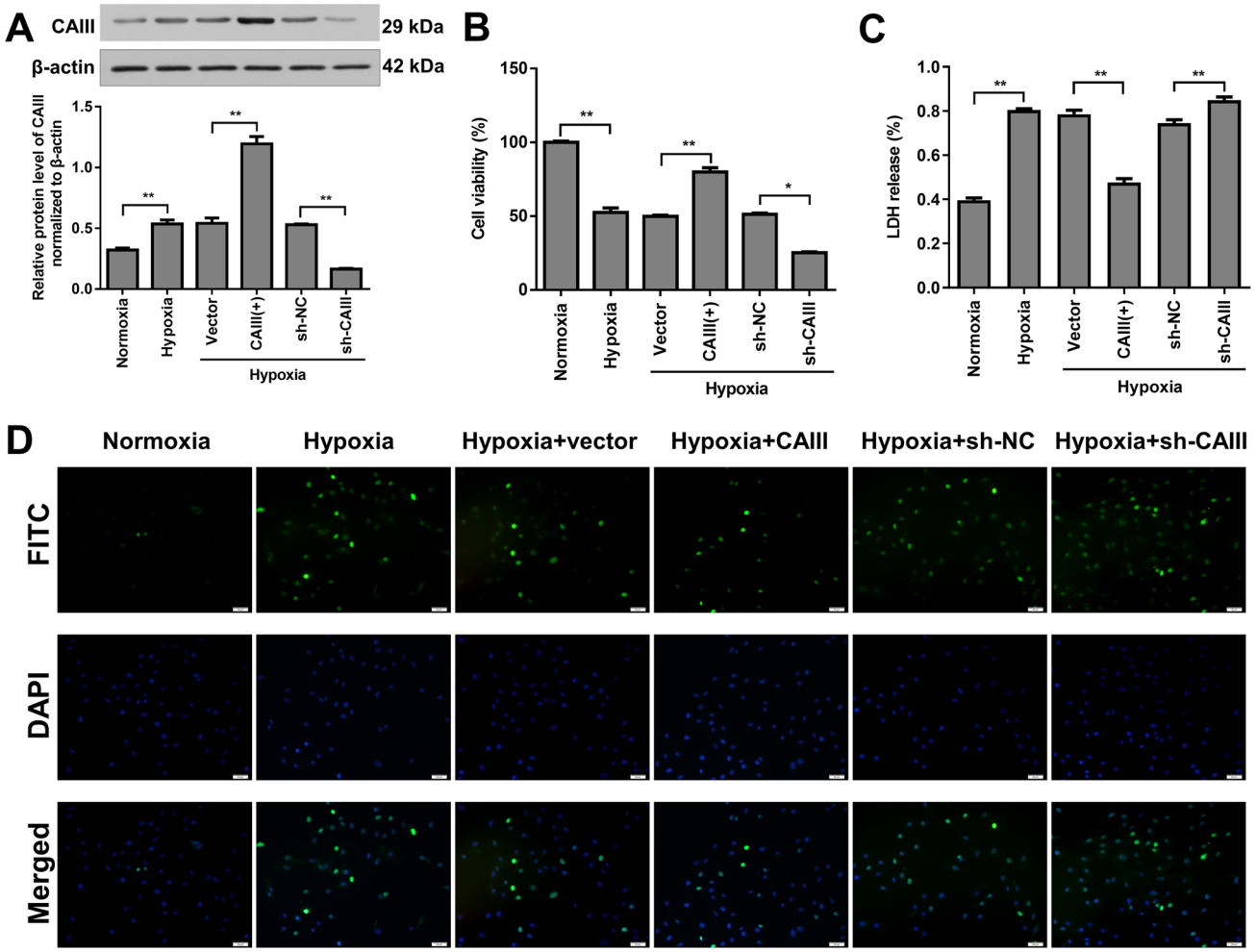

Fig. 4 Apoptotic status after 24 h were detected in normoxia, hypoxia, hypoxia + vector, hypoxia + CAIII(+), hypoxia + sh-NC, and hypoxia + sh-CAIII group. **A** Relative expression of CAIII protein via normalized to β-actin expression. **B** H9c2 cell viability was detected by MTT assay. **C** LDH release was detected by Cytotoxicity Assay Commercial kits. **D** The content of apoptotic H9c2 cells was observed by TUNEL assay (scale bar = 50 μm). The green dots referred to apoptotic cells and blue referred to DAPI, stained cells included apoptotic and live cells. $^{*}P < 0.05$ between two groups; $^{**}P < 0.01$ between two groups

100 target genes related to hypoxic adaptation, inflammation development, and tumor growth. It could be quickly degraded by cells under aerobic conditions, but stably expressed only under hypoxic conditions. A previous study found that there was significant overlapping existed between overexpression of HIF-1α and carbonic anhydrase [33]. The activation of PI3K/Akt/mTOR pathway, which played a regulatory role in multiple physiological functions including cell growth, differentiation, and autophagy, was reported to be regulated by HIF-1α [34]. The activated PI3K could be propagated to various substrates that included mTOR, a master regulator of protein translation, while the activated Akt could regulate cell functions by phosphorylating downstream factors including various enzymes and transcription factors [35]. Shen et al. demonstrated that HIF-1α participated in the expression of PI3K and the phosphorylation of Akt [36]. Another publication also indicated that expression of PI3K/Akt and mTOR/p70S6K1 signaling participated in the activation of HIF-1α [37]. Meanwhile, the expression of PI3K/Akt/mTOR and their phosphorylated proteins contribute to attenuating apoptosis of human colorectal cancer cells [38]. Our western blotting results indicated that the level of HIF-1α was increased under hypoxia treatment and could be further upregulated by overexpression of CAIII, in which, the activated PI3K/Akt/mTOR pathway may also be participated.

A previous study reported that CAIX could interact with Dickkopf-1, a negative regulator of the Wnt signaling pathway, and further induced CAIX-mediated mTOR phosphorylation in human cervical carcinoma cells [39]. Moreover, CAIII was demonstrated to enhance oral cancer cells migration ability through FAK/Src pathway, where

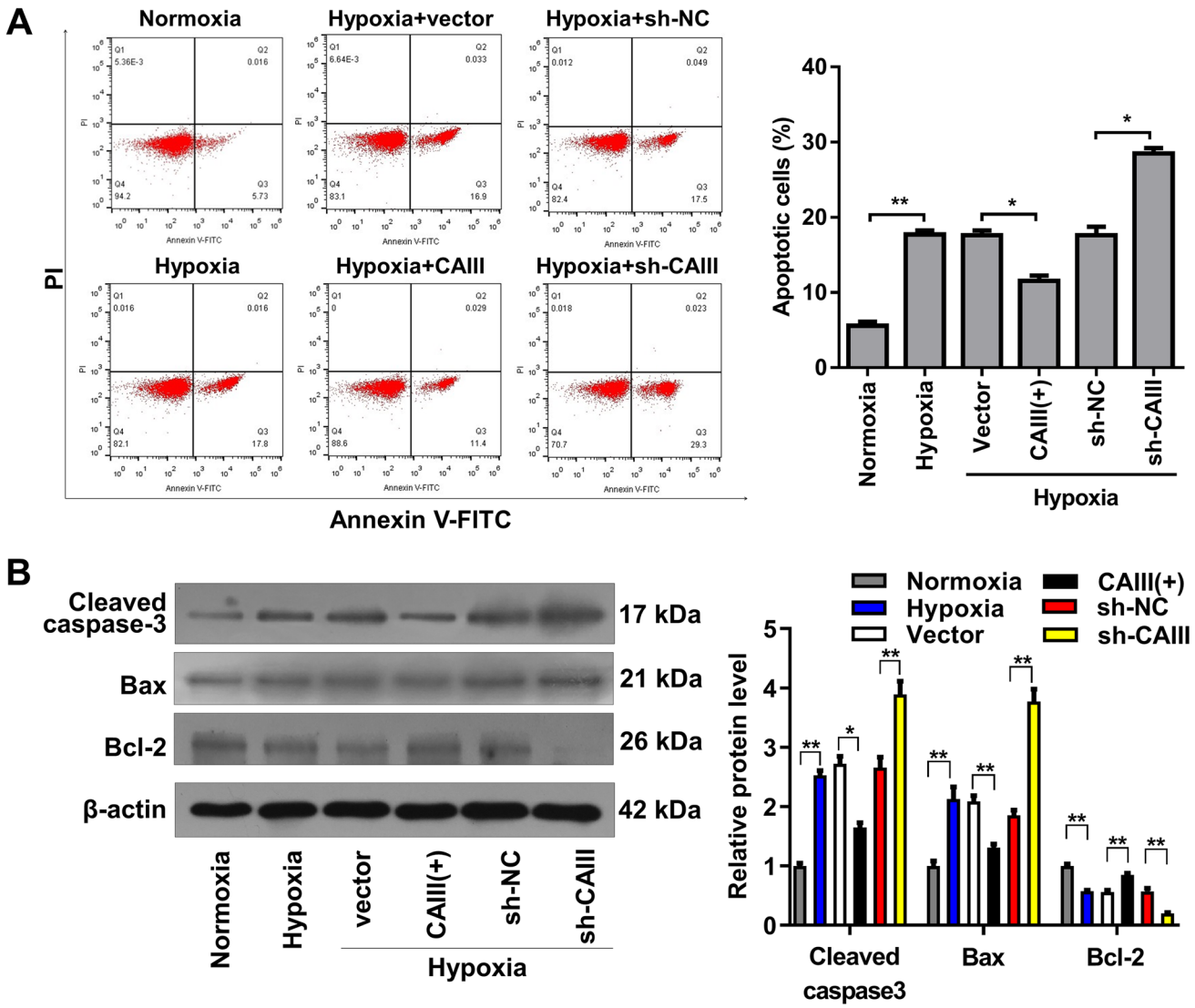

Fig. 5 Levels of apoptosis-related proteins were detected in normoxia, hypoxia, hypoxia + vector, hypoxia + CAIII(+), hypoxia + sh-NC, and hypoxia + sh-CAIII groups. **A** The content of apoptotic H9c2 cells was determined by flow cytometric analysis. **B** Levels of cleaved caspase-3, Bcl-2, and Bax were determined by western blotting. The relative expression was calculated via normalized to β-actin expression. $^{*}P < 0.05$, $^{**}P < 0.01$ between two groups

the overexpression of CAIII promoted the phosphorylation of FAK and Src, while inhibiting CAIII using siRNA significantly decreased the p-FAK and p-Src levels [40]. Similarly, the CAIII transfectants elevated the FAK and Src activity in hepatoma cells and contributed to its transformation and invasion capability, indicating that CAIII potentially regulated the FAK expression and affected the downstream PI3K/Akt/mTOR pathway [41]. In the present study, we found that overexpression of CAIII significantly activated the PI3K/Akt/mTOR pathway, suggesting the possible role of PI3K/Akt/mTOR in CAIII-mediated attenuation of hypoxia-induced apoptosis in H9c2 cardiomyocytes. However, whether CAIII could directly interact with PI3K/Akt/mTOR pathway or through its upstream genes such as FAK or Janus kinase pathways still needs further investigation.

In summary, this study aimed at elucidating the protection role of CAIII in hypoxia-induced cell apoptosis in sheep myocardial tissues and provided newly theoretical reference for therapy of hypoxia-induced injury. Moreover, other proteins related to protective function from hypoxia including REN, IGHM, APOBEC 3F, and SKOR2 could also be explored in-depth in the future, presenting an overall insight of the mechanism by which CAIII was regulated.

In the current study, we discovered that overexpression of CAIII could protect cell from apoptosis caused by hypoxia in H9c2 cells and alleviate cytotoxicity via upregulating HIF-1α level and stimulating PI3k/Akt/

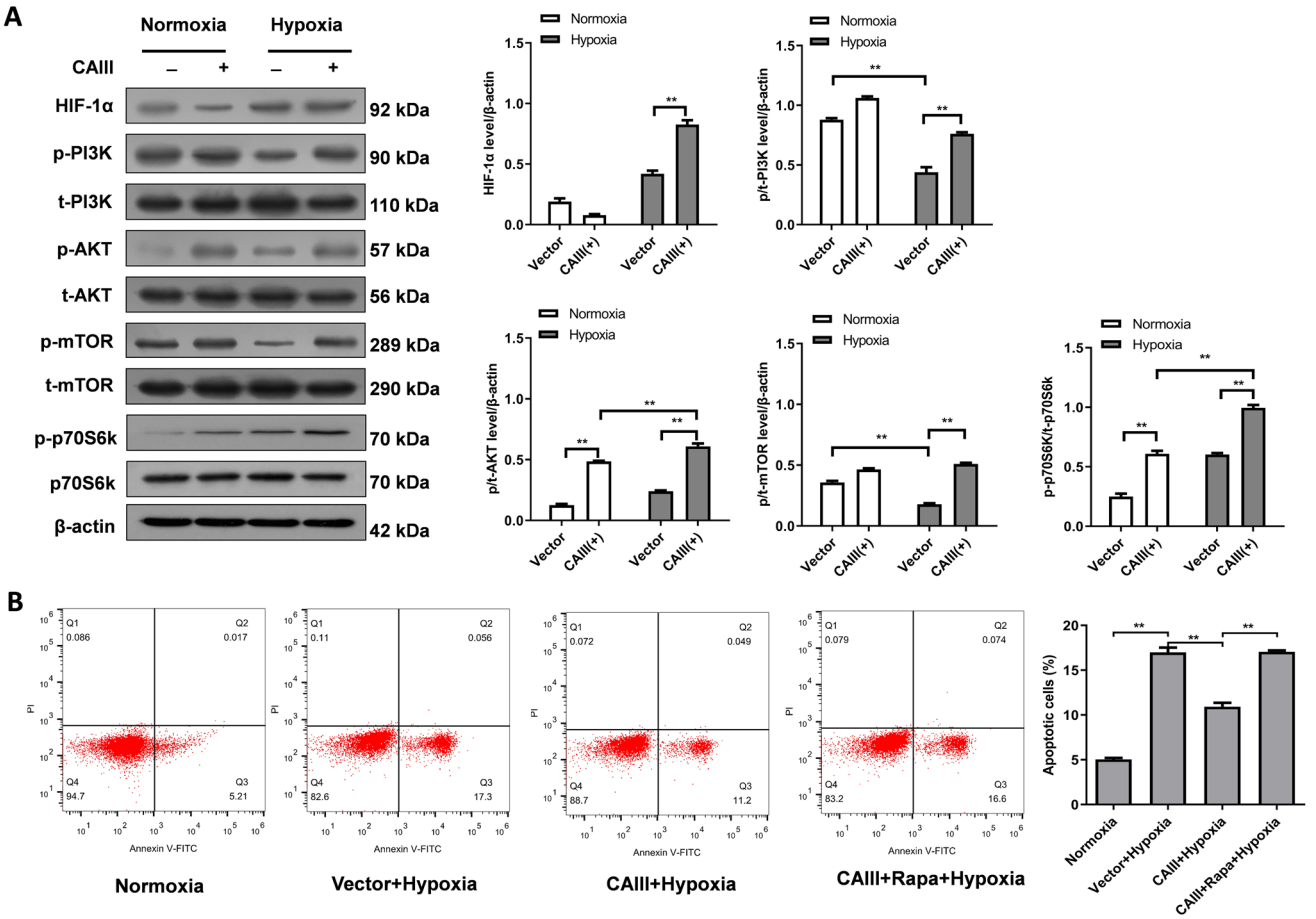

Fig. 6 **A** Protein levels of HIF-1α, p-PI3K, t-PI3K, p-Akt, t-Akt, p-mTOR, t-mTOR, p-p70S6K, and t-p70S6K in normoxia and hypoxia groups were detected by western blotting. The relative expression of HIF-1α, p/t-PI3K, p/t-Akt, p/t-mTOR, and p/t-p70S6K was calculated via normalization to β-actin expression. **B** The apoptosis of H9c2 cells with indicated treatment was detected using flow cytometry. The apoptosis was significantly increased under treatment with specific mTOR inhibitors. $^{**}P < 0.01$ between groups. *P* phosphorylated, *t* total

mTOR pathway. Thus, CAIII might be a potential therapeutic target for the development of treating hypoxia-induced damage.

Author contributions HL conceived and designed the entire study; HL and YBL collected and analyzed the data, and they were responsible for data interpretation; they were co-first authors; ST, JH, QLW, YW, and MN performed statistical analysis, literature research, and data visualization; HL and YBL wrote the manuscript. HL revised it critically for important intellectual content. All authors have read and approved the final manuscript.

Funding This research was supported by "The effects of hypoxia during pregnancy on fetal cardiovascular development and its related mechanisms" (Grant No.: 81560291).

Data availability All data generated or analyzed during this study are included in this manuscript.

Declarations

Conflict of interest The authors declare that they have no competing interests.

Ethical approval This study was approved by the Ethics Committee of General Hospital of Xinjiang Military Region of the People's Liberation Army (No. 2017.301).

References

1. Gulati, R., Behfar, A., Narula, J., Kanwar, A., Lerman, A., Cooper, L., & Singh, M. (2020). Acute myocardial infarction in young individuals. *Mayo Clinic Proceedings, 95*, 136–156.
2. Li, M., Ding, W., Tariq, M. A., et al. (2018). A circular transcript of ncx1 gene mediates ischemic myocardial injury by targeting miR-133a-3p. *Theranostics, 8*, 5855–5869.

3. Han, D., Wang, Y., Chen, J., et al. (2019). Activation of melatonin receptor 2 but not melatonin receptor 1 mediates melatonin-conferred cardioprotection against myocardial ischemia/reperfusion injury. *Journal of Pineal Research, 67*, e12571.
4. Penaloza, D., & Arias-Stella, J. (2007). The heart and pulmonary circulation at high altitudes: Healthy highlanders and chronic mountain sickness. *Circulation, 115*, 1132–1146.
5. Wang, Y., Zhao, Z., Zhu, Z., Li, P., Li, X., Xue, X., Duo, J., & Ma, Y. (2018). Telomere elongation protects heart and lung tissue cells from fatal damage in rats exposed to severe hypoxia. *Journal of Physiological Anthropology, 37*, 5.
6. Innocenti, A., Scozzafava, A., Parkkila, S., Puccetti, L., De Simone, G., & Supuran, C. T. (2008). Investigations of the esterase, phosphatase, and sulfatase activities of the cytosolic mammalian carbonic anhydrase isoforms I, II, and XIII with 4-nitrophenyl esters as substrates. *Bioorganic & Medicinal Chemistry Letters, 18*, 2267–2271.
7. Zebral, Y. D., da Silva, F. J., Marques, J. A., & Bianchini, A. (2019). Carbonic anhydrase as a biomarker of global and local impacts: Insights from calcifying animals. *International Journal of Molecular Sciences, 20*, 3092.
8. Shang, X., Chen, S., Ren, H., Li, Y., & Huang, H. (2009). Carbonic anhydrase III: The new hope for the elimination of exercise-induced muscle fatigue. *Medical Hypotheses, 72*, 427–429.
9. Lippi, G., Schena, F., Montagnana, M., Salvagno, G. L., & Guidi, G. C. (2008). Influence of acute physical exercise on emerging muscular biomarkers. *Clinical Chemistry and Laboratory Medicine, 46*, 1313–1318.
10. Ren, H. M., Jiang-Long, T. U., Ai-Lian, D. U., & Huang, J. (2005). Demonstration of carbonic anhydrase III for 25 000 protein decreased in skeletal muscle of myasthenia gravis. *Chinese Journal of Neurology, 38*, 764–768.
11. Zoll, J., Ponsot, E., Dufour, S., et al. (2006). Exercise training in normobaric hypoxia in endurance runners. III. Muscular adjustments of selected gene transcripts. *Journal of Applied Physiology, 100*, 1258–1266.
12. Engelman, J. A. (2009). Targeting PI3K signalling in cancer: Opportunities, challenges and limitations. *Nature Reviews Cancer, 9*, 550–562.
13. Zhang, Y., Zhang, J. W., Lv, G. Y., Xie, S. L., & Wang, G. Y. (2012). Effects of STAT3 gene silencing and rapamycin on apoptosis in hepatocarcinoma cells. *International Journal of Medical Sciences, 9*, 216–224.
14. Jalde, F. C., Jalde, F., Sackey, P. V., et al. (2016). Neurally adjusted ventilatory assist feasibility during anaesthesia: A randomised crossover study of two anaesthetics in a large animal model. *European Journal of Anaesthesiology, 33*(4), 283–291.
15. Schill, M. R., Melby, S. J., Speltz, M., Breitbach, M., Schuessler, R. B., & Damiano, R. J., Jr. (2017). Evaluation of a novel cryoprobe for atrial ablation in a chronic ovine model. *Annals of Thoracic Surgery, 104*, 1069–1073.
16. Cicero, L., Fazzotta, S., Palumbo, V. D., et al. (2014). Anesthesia protocols in laboratory animals used for scientific purposes. *Journal of the American Association for Laboratory Animal Science, 53*(3), 290–300.
17. Fernando, S. C., Adriano, B. C., Alceu, G. R., et al. (2010). Total intravenous anesthesia with propofol and S(+)-ketamine in rabbits. *Veterinary Anaesthesia and Analgesia, 37*(2), 116–22.
18. Dileep, K., Gauhar, A., Muhammad, Z., et al. (2019). Isoflurane alone versus small dose propofol with isoflurane for removal of laryngeal mask airway in children-A randomized controlled trial. *The Journal of the Pakistan Medical Association, 69*(11), 1596–1600.
19. Tanya, D. N., Carolina, P. J., Tara, W., et al. (2015). Cardiopulmonary effects of dexmedetomidine and ketamine infusions with either propofol infusion or isoflurane for anesthesia in horses. *Veterinary Anaesthesia and Analgesia, 42*(1), 39–49.
20. Yang, J., Chen, L., Ding, J., et al. (2016). Cardioprotective effect of miRNA-22 on hypoxia/reoxygenation induced cardiomyocyte injury in neonatal rats. *Gene, 579*, 17–22.
21. Faridvand, Y., Nozari, S., et al. (2018). Nrf2 activation and downregulation of HMGB1 and MyD88 expression by amnion membrane extracts in response to the hypoxia-induced injury in cardiac H9c2 cells. *Biomedecine & Pharmacotherapie, 109*, 360.
22. Li, H., Hu, J., Liu, Y., et al. (2018). Effects of prenatal hypoxia on fetal sheep heart development and proteomics analysis. *International Journal of Clinical and Experimental Pathology, 11*, 1909–1922.
23. Zhao, T., Fu, Y., Sun, H., & Liu, X. (2018). Ligustrazine suppresses neuron apoptosis via the Bax/Bcl-2 and caspase-3 pathway in PC12 cells and in rats with vascular dementia. *IUBMB Life, 70*, 60–70.
24. Yeung, H. M., Hung, M. W., Lau, C. F., & Fung, M. L. (2015). Cardioprotective effects of melatonin against myocardial injuries induced by chronic intermittent hypoxia in rats. *Journal of Pineal Research, 58*, 12–25.
25. Staunton, L., Zweyer, M., Swandulla, D., & Ohlendieck, K. (2012). Mass spectrometry-based proteomic analysis of middle-aged vs. aged vastus lateralis reveals increased levels of carbonic anhydrase isoform 3 in senescent human skeletal muscle. *International Journal of Molecular Medicine, 30*, 723–733.
26. Vaananen, H. K., Syrjala, H., Rahkila, P., et al. (1990). Serum carbonic anhydrase III and myoglobin concentrations in acute myocardial infarction. *Clinical Chemistry, 36*, 635–638.
27. Zhao, X., Wang, K., Hu, F., et al. (2015). MicroRNA-101 protects cardiac fibroblasts from hypoxia-induced apoptosis via inhibition of the TGF-beta signaling pathway. *International Journal of Biochemistry & Cell Biology, 65*, 155–164.
28. Lu, Z., Li, S., Zhao, S., & Fa, X. (2016). Upregulated miR-17 regulates hypoxia-mediated human pulmonary artery smooth muscle cell proliferation and apoptosis by targeting mitofusin 2. *Medical Science Monitor, 22*, 3301–3308.
29. Shang, X., Bao, Y., Chen, S., Ren, H., Huang, H., & Li, Y. (2012). Expression and purification of TAT-fused carbonic anhydrase III and its effect on C2C12 cell apoptosis induced by hypoxia/reoxygenation. *Archives of Medical Science AMS, 4*, 711–718.
30. Wu, X., Hao, C., Ling, M., Guo, C., & Ma, W. (2015). Hypoxia-induced apoptosis is blocked by adrenomedullin via upregulation of Bcl-2 in human osteosarcoma cells. *Oncology Reports, 34*, 787–794.
31. Pan, Y. L., Han, Z. Y., He, S. F., et al. (2018). miR133b5p contributes to hypoxic preconditioningmediated cardioprotection by inhibiting the activation of caspase8 and caspase-3 in cardiomyocytes. *Molecular Medicine Reports, 17*, 7097–7104.
32. Eldehna, W. M., Abo-Ashour, M. F., Nocentini, A., et al. (2017). Novel 4/3-((4-oxo-5-(2-oxoindolin-3-ylidene)thiazolidin-2-ylidene)amino) benzenesulfonamides: Synthesis, carbonic anhydrase inhibitory activity, anticancer activity and molecular modelling studies. *European Journal of Medicinal Chemistry, 139*, 250–262.
33. Saenz-de-Santa-Maria, I., Bernardo-Castineira, C., Secades, P., et al. (2017). Clinically relevant HIF-1alpha-dependent metabolic reprogramming in oropharyngeal squamous cell carcinomas includes coordinated activation of CAIX and the miR-210/ISCU signaling axis, but not MCT1 and MCT4 upregulation. *Oncotarget, 8*, 13730–13746.
34. Giacoppo, S., Bramanti, P., & Mazzon, E. (2017). Triggering of inflammasome by impaired autophagy in response to acute experimental Parkinson's disease: Involvement of the PI3K/Akt/mTOR pathway. *NeuroReport, 28*, 996–1007.

35. LoPiccolo, J., Blumenthal, G. M., Bernstein, W. B., & Dennis, P. A. (2008). Targeting the PI3K/Akt/mTOR pathway: Effective combinations and clinical considerations. *Drug Resistance Updates, 11*, 32–50.
36. Shen, W., Cheng, K., Bao, Y., Zhou, S., & Yao, H. (2012). Expression of Glut-1, HIF-1α, PI3K and p-Akt in a case of ceruminous adenoma. *Head & Neck Oncology, 4*, 18.
37. Agani, F., & Jiang, B. H. (2013). Oxygen-independent regulation of HIF-1: Novel involvement of PI3K/AKT/mTOR pathway in cancer. *Current Cancer Drug Targets, 13*, 245–251.
38. Yang, L., Liu, Y., Wang, M., et al. (2016). Celastrus orbiculatus extract triggers apoptosis and autophagy via PI3K/Akt/mTOR inhibition in human colorectal cancer cells. *Oncology Letters, 12*, 3771–3778.
39. Kim, B. R., Shin, H. J., Kim, J. Y., Byun, H. J., Lee, J. H., Sung, Y. K., & Rho, S. B. (2012). Dickkopf-1 (DKK-1) interrupts FAK/PI3K/mTOR pathway by interaction of carbonic anhydrase IX (CA9) in tumorigenesis. *Cellular Signalling, 24*, 1406–1413.
40. Chu, Y. H., Su, C. W., Hsieh, Y. S., Chen, P. N., Lin, C. W., & Yang, S. F. (2020). Carbonic anhydrase III promotes cell migration and epithelial-mesenchymal transition in oral squamous cell carcinoma. *Cells, 9*, 704.
41. Dai, H. Y., Hong, C. C., Liang, S. C., Yan, M. D., Lai, G. M., Cheng, A. L., & Chuang, S. E. (2008). Carbonic anhydrase III promotes transformation and invasion capability in hepatoma cells through FAK signaling pathway. *Molecular Carcinogenesis, 47*, 956–963.